ACADEMIC PRESS

Available online at www.sciencedirect.com

SCIENCE DIRECT®

Journal of Sound and Vibration 270 (2004) 1–14

JOURNAL OF SOUND AND VIBRATION

www.elsevier.com/locate/jsvi

# Damage detection in structures using a few frequency response measurements

H.Y. Hwang[a,*], C. Kim[b]

[a] *Department of Aerospace Engineering, Sejong University, 98 Kwangjin-Gu, Kunja-dong, Seoul 143-747, South Korea*
[b] *School of Mechanical Engineering, Kyungpook National University, Daegu 702-701, South Korea*

Received 22 January 2002; accepted 4 February 2003

**Abstract**

This paper presents methods to identify the locations and severity of damage in structures using frequency response function (FRF) data. Basic methods detect the location and severity of structural damage by minimizing the difference between test and analytic FRFs, which is a type of model updating or optimization method; however, the preferred method proposed in this paper uses only a subset of vectors from the full set of FRFs for a few frequencies and calculates the stiffness matrix and reductions in explicit form. To verify the proposed method, examples for a simple cantilever and a helicopter rotor blade are numerically demonstrated. The proposed method identified the location of damage in these objects, and characterized the damage to a satisfactory level of precision.


## 1. Introduction

The problem of monitoring the structural health of an object consists of obtaining information about the existence, location, and extent of damage in the structure using non-destructive methods. One approach is to monitor and interpret changes in structural dynamic measurements based on experimental modal analyses and signal-processing techniques. The extraction of the natural frequency and mode shape of a vibrating structure can be accomplished using modern vibration testing equipment and instrumentation. The modal and structural dynamic data can then be utilized for cost-effective health monitoring and operational life assessment without requiring the structure to be dismantled [1].

*Corresponding author. Tel.: +82-2-3408-3773; fax: +82-2-3408-3333.
*E-mail address:* hyhwang@sejong.ac.kr (H.Y. Hwang).

0022-460X/03/$ - see front matter 
doi:10.1016/S0022-460X(03)00190-1

A general approach for detecting damage, proposed by several researchers [2–15], is based on comparing the frequency changes obtained using experimental data collected from the structure with the sensitivity of the modal parameters obtained from an analytical model of the structure. The sensitivity of the natural frequencies of the structure to changes in the stiffness, mass, and damping are calculated using a finite element analysis. However, methods based on a sensitivity analysis require an accurate analytical model of the structure being investigated, which can be difficult to obtain. Also, most of the damage detection algorithms require a significant amount of modal test data. These requirements make the damage detection procedure expensive, time-consuming, and impractical for real-life structures in service.

Abdalla et al. [1] formulated the damage detection problem as a convex optimization problem involving linear matrix inequality constraints. Pandey et al. [2] presented an evaluation of changes in the structure flexibility matrix as a candidate method for identifying both the presence and the location of the damage. Farhat et al. [3] developed a sensitivity-based methodology for improving the finite element model of a given structure using test modal data and a few sensors. Li et al. [5] used modal characteristics extracted from vibration tests with an original finite element model in an identification approach developed to combine the advantages of two classes of techniques: eigensensitivity and multiple-constraint matrix adjustment. Smith [7] applied alternating projection algorithms for approximating a matrix in structural model updating. The desired matrix properties, such as sparsity, definiteness, and the satisfaction of eigenconstraints, were imposed as side constraints for a minimization problem formulated to produce an updated matrix model that better matched the measured data. Ahmadian et al. [8] addressed the problem of selecting a side constraint and determining the regularization parameter when updating the model; the constraint weight was determined by the regularization parameter. They considered methods based on singular value decomposition, cross-validation, and L-curves.

In this paper, structural damage was detected using techniques based on the physical meaning of the stiffness matrices and on a few frequency response functions (FRFs) that can be obtained from a test. The basis for this method is that damage produces a decrease in the dynamic stiffness $EI$. The symmetry and physical properties of the stiffness matrices were maintained by considering their sparsity.

Despite the presence of experimental errors in the FRF test data, it is generally assumed that this data is a better representation of how the structure behaves than the initial predictions from the FE model. Consequently, in this paper, it is assumed that to the FE model was adjusted, or updated, so that the results it produces are in some sense closer to the experimental results.

There has been a significant amount of work on generating and testing different updating methods over the past 20 years. The resulting algorithms may be split into several categories based on whether they work in the frequency or modal domains and whether they adjust the mass and stiffness matrices directly (direct methods) or make parametric changes to the model (indirect or parametric methods) [7].

Although it is fairly easy to detect the presence of damage in a structure from changes in the natural frequencies, it is difficult to determine the location of the damage. This is because damage at two different locations may produce the same amount of frequency change. Previous research [2–12] based on modal methods that use the natural frequency and modal shape changes should not be used in damage assessment methodologies because the modal shapes of a damaged and

undamaged system are nearly the same. Hence, in this paper, FRFs are used to detect damage, rather that the natural frequencies and modal shapes.

In this paper, to reduce the computational time required to analyze a structure that has been damaged at more than one location, two FRFs were used iteratively for different frequency values. This created a large number of equations to accurately identify the damage, and eliminated the need for a large amount of FRF data. The method worked for each discrete frequency and could be optimized using the least-squares method. The damage detection equation was rearranged to avoid ill-conditioned problems while the matrices were being inverted. The *EI* stiffness values were separated from the element stiffness matrix when using the least-squares method; this minimized the number of unknowns in the stiffness matrix and preserved the intrinsic FEM connectivity properties of the model. The derived damage detection method was tested on a simple cantilever and a helicopter rotor blade.

## 2. Formulation of the equations of motion

Damage will alter the dynamic characteristics of a structure. This is characterized by changes in the modal parameters, i.e., the modal frequencies, damping values, and mode shapes associated with each modal frequency. Changes also occur in some of the structural parameters, such as the mass, damping, stiffness, and flexibility matrices of the structure.

The equations of motion of a structure with $N$ degrees of freedom and viscous damping coefficients can be expressed as [16]

$$[M]\{\ddot{x}(t)\} + [D]\{\dot{x}(t)\} + [K]\{x(t)\} = \{f(t)\}, \tag{1}$$

where $[M]$, $[D]$, and $[K]$ represent the $n \times n$ mass, damping, and stiffness matrices. If we assume a harmonic input, the external force and displacement can be expressed as $\{f(t)\} = \{F(\omega)\}e^{j\omega t}$ and $\{x(t)\} = \{X(\omega)\}e^{j\omega t}$. Substituting into Eq. (1) yields

$$(-\omega^2[M] + j\omega[D] + [K])\{X(\omega)\}e^{i\omega t} = \{F(\omega)\}e^{i\omega t}. \tag{2}$$

From the above equation, the FRF matrix, $[H(\omega)]$, is defined as

$$[H(\omega)] = (-\omega^2[M] + j\omega[D] + [K])^{-1}. \tag{3}$$

Then Eq. (2) can be expressed as

$$\{X(\omega)\} = [H(\omega)]\{F(\omega)\}. \tag{4}$$

## 3. Damage detection methods using FRF data

The objective of this paper is to identify the location and amount of structural damage, which is related to the stiffness matrices. Therefore, the damping matrix $[D]$ in Eq. (1) is neglected even though damping reduces the natural frequency slightly. Small local changes in the mass of a beam can cause significant changes in the frequency. Hence, we also assume that the mass of the structure does not change after it has been damaged. We assign the damaged part of the structure to the connection between two substructures, illustrated in Fig. 1.


Fig. 1. Damaged structure divided into two substructures.

The stiffness matrix of the damaged part can then be obtained from

$$[K]_{unknown} = ([K] - \omega^2[M]) - ([K]_{new} - \omega^2[M]), \tag{5}$$

where $[K]$ is the stiffness matrix of the structure without damage, and $[K]_{new} = [K]_{\mathrm{I}} + [K]_{\mathrm{II}}$ is composed of the stiffness matrices of substructure I and II without connections, i.e.,

$$[K]_{new} = \begin{bmatrix} [K]_{\mathrm{I}} & [0] \\ [0] & [0] \end{bmatrix} + \begin{bmatrix} [0] & [0] \\ [0] & [K]_{\mathrm{II}} \end{bmatrix}. \tag{6}$$

The subscript 'unknown' indicates the stiffness value of the damaged parts in the structure.

Using the relation $[H(\omega)]^{-1} = ([K] - \omega^2[M])$ and Eq. (5), we can theoretically obtain the stiffness matrix for the damaged portion of the structure by subtracting the inverse of the FRF with damage from the inverse of the FRF without damage. However, this method requires a large number of calculations because many sub-stiffness matrices must be calculated continuously due to the damaged points. Also, one needs to measure all the modes of the structure, especially the high-frequency modes, to obtain a good estimate of the stiffness matrix. Because of obvious limitations in experimental instrumentation, it becomes increasingly difficult to measure the higher frequency response data. Hence, to find the location and amount of damage using just a few test data, it is necessary to iterate the calculations using both the theoretical FRFs from the finite element model and the experimental FRFs. However, only a few lower frequency modes need to be measured to generate the necessary stiffness matrices.

In Eq. (3), if damping is neglected, the FRFs matrix can be expressed as

$$[H(\omega)] = (-\omega^2[M] + [K])^{-1}. \tag{7}$$

Let the FRFs from the test be $[H(\omega)]_T$. Using the mass matrix ($[M]_A$) and the stiffness matrix ($[K]_A$) from the finite element model, the simulated FRFs are

$$[H(\omega)]_A = (-\omega^2[M]_A + [K]_A)^{-1}. \tag{8}$$

When a structure contains damage, $[H(\omega)]_T$ differs from $[H(\omega)]_A$ due to the stiffness reduction. Hence, we can find the location and amount of damage through iterations by matching $[H(\omega)]_T$ to $[H(\omega)]_A$. This basic computational scheme is illustrated in Fig. 2. However, in practice, these calculations are extremely difficult to perform because of the matrix inverting process, which may introduce highly ill-posed problems.

This method was tested using a simple discrete model with six degrees of freedom. The most reliable $1/\sqrt{2}$ of the peak FRF values were used to compare $[H(\omega)]_T$ and $[H(\omega)]_A$. In practical applications, the measurements will include errors arising from many potential sources; therefore, errors in the amplitude measurement of the FRFs were considered. An intentional 10% random noise error was added to simulate noise effects. During the iterative process, according to the scheme shown in Fig. 2, 1% of the stiffness values were reduced in the undamaged $[K]$.

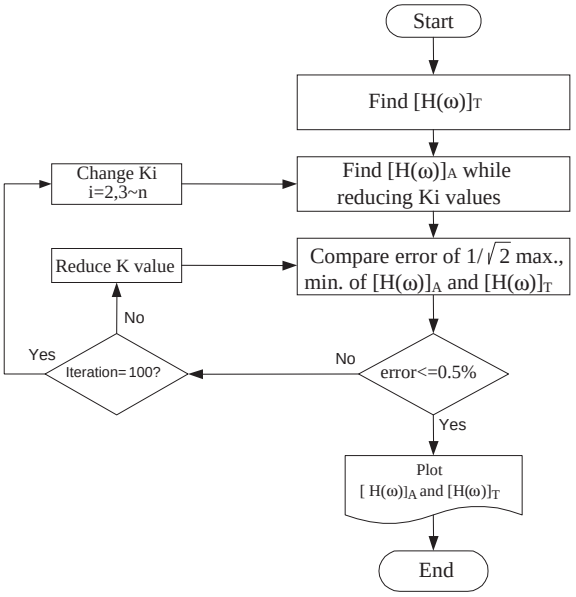


Fig. 2. Computational scheme for the basic method.

The FRFs at different iteration times during the reduction of one spring constant value are shown in Fig. 3. As the iteration number increases, $[H(\omega)]_A$ approaches $[H(\omega)]_T$ and the spring constant is reduced to the value that was assumed in the damaged structure.

The above method can be used to find the position and the amount of damage at one element using just one FRF. However, for structures that have been damaged at more than one element, we have to compare the test FRF to analytical FRFs obtained using different combinations of the sub-stiffness matrices. This makes the method difficult to apply due to the sharp increase in the amount of calculations that are required. Therefore, a new approach is introduced that uses a specific FRF and iterates for different frequencies.

From Eq. (7), the test FRF is

$$[H(\omega)]_T = (-\omega^2[M] + [K]_T)^{-1}. \tag{9}$$

Rearranging the above equation yields $[K]_T = [H]_T^{-1} + \omega^2[M]$. However, it is extremely difficult to obtain $[H]_T^{-1}$ because we cannot measure all the FRFs, and the inversion process creates ill-conditioned problems. Therefore, a new method is required that locates the damaged position using just a few test sets. From Eq. (9), $[H(\omega)]_T(-\omega^2[M] + [K]_T) = [I]$, which can be expressed in detail as

$$\begin{bmatrix} H_{11}(\omega) & H_{12}(\omega) & \cdot & \cdot & H_{1n}(\omega) \\ H_{21}(\omega) & H_{22}(\omega) & \cdot & \cdot & H_{2n}(\omega) \\ \cdot & \cdot & \cdot & \cdot & \cdot \\ \cdot & \cdot & \cdot & \cdot & \cdot \\ H_{n1}(\omega) & H_{n2}(\omega) & \cdot & \cdot & H_{nn}(\omega) \end{bmatrix}_T \begin{bmatrix} T_{11}(\omega) & T_{12}(\omega) & \cdot & \cdot & T_{1n}(\omega) \\ T_{21}(\omega) & T_{22}(\omega) & \cdot & \cdot & T_{2n}(\omega) \\ \cdot & \cdot & \cdot & \cdot & \cdot \\ \cdot & \cdot & \cdot & \cdot & \cdot \\ T_{n1}(\omega) & T_{n2}(\omega) & \cdot & \cdot & T_{nn}(\omega) \end{bmatrix} = \begin{bmatrix} 1 & 0 & \cdot & \cdot & 0 \\ 0 & 1 & \cdot & \cdot & 0 \\ \cdot & \cdot & \cdot & \cdot & \cdot \\ \cdot & \cdot & \cdot & \cdot & \cdot \\ 0 & 0 & \cdot & \cdot & 1 \end{bmatrix}_{n\times n}, \tag{10}$$

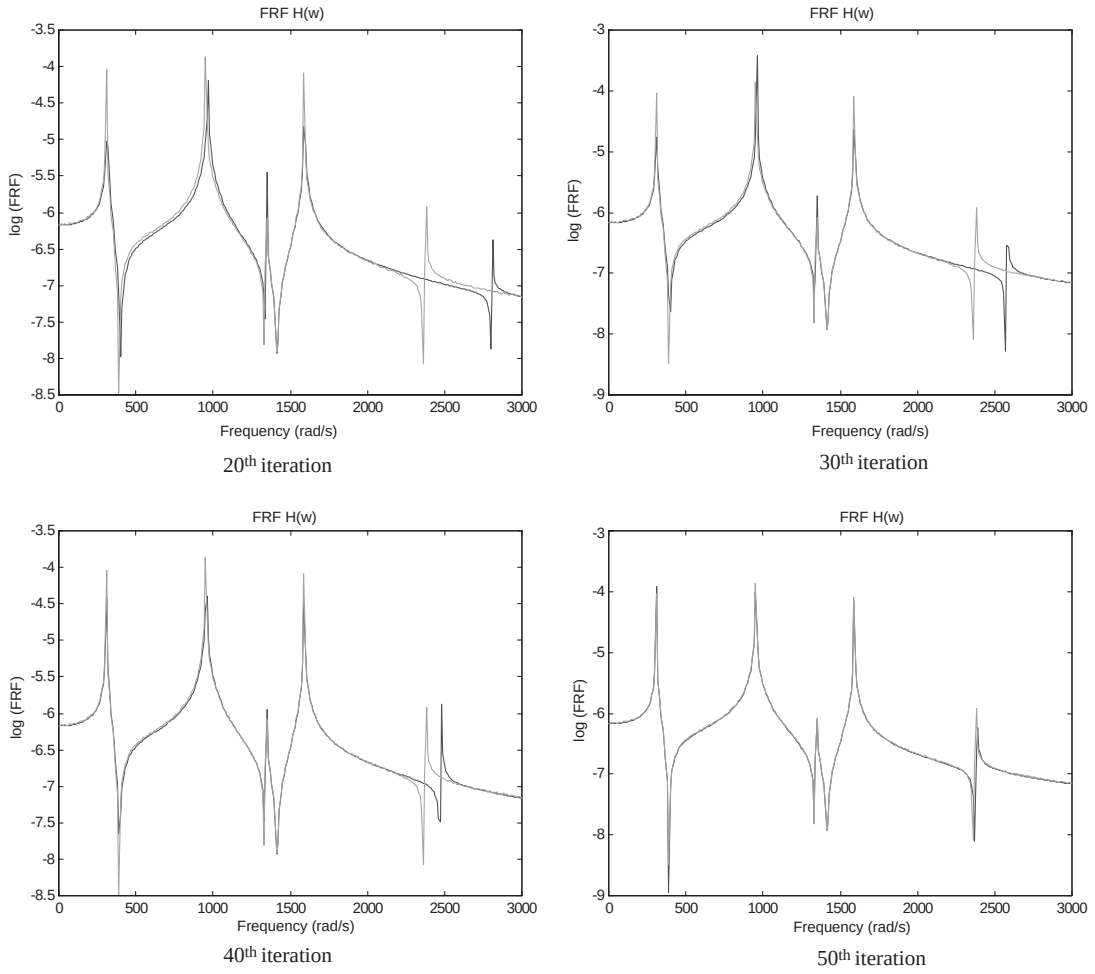


Fig. 3. FRFs at different iteration times.

where $[T] = ([K]_T - \omega^2[M])$. This expression is frequency dependent rather than a constant. For a specific $x$th row of $[H]_T$, we can obtain the $1 \times n$ matrix

$$[\,H_{x1} \quad H_{x2} \quad \cdot \quad H_{xn}\,]_T([K_T])_{n\times n} = [\,0 \quad \ldots \quad 010 \quad \ldots \quad 0\,] + \omega^2[\,H_{x1} \quad H_{x2} \quad \cdot \quad H_{xn}\,]_T[M]_{n\times n}$$

by rearranging the above equation. However, its inverse matrix cannot be determined uniquely to give $[K]_T$. Thus, the above equation is used iteratively for different frequencies, $\omega_i$. This provides a sufficient number of equations using the least-squares method.

If we consider the first row, the different $n$ frequencies yield to the following equation:

$$\begin{bmatrix} H_{11}(\omega_1) & H_{12}(\omega_1) & \cdot & \cdot & H_{1n}(\omega_1) \\ H_{11}(\omega_2) & H_{12}(\omega_2) & \cdot & \cdot & H_{1n}(\omega_2) \\ \cdot & \cdot & \cdot & \cdot & \cdot \\ \cdot & \cdot & \cdot & \cdot & \cdot \\ H_{11}(\omega_n) & H_{12}(\omega_n) & \cdot & \cdot & H_{1n}(\omega_n) \end{bmatrix}_T \begin{bmatrix} K_{11} & K_{12} & \cdot & \cdot & K_{1n} \\ K_{21} & K_{22} & \cdot & \cdot & K_{2n} \\ \cdot & \cdot & \cdot & \cdot & \cdot \\ \cdot & \cdot & \cdot & \cdot & \cdot \\ K_{n1} & K_{n2} & \cdot & \cdot & K_{nn} \end{bmatrix}_T = \begin{bmatrix} 1 & 0 & \cdot & \cdot & 0 \\ 1 & 0 & \cdot & \cdot & 0 \\ \cdot & \cdot & \cdot & \cdot & \cdot \\ \cdot & \cdot & \cdot & \cdot & \cdot \\ 1 & 0 & \cdot & \cdot & 0 \end{bmatrix}$$

$$+ \begin{bmatrix} \ddots & & \\ & \omega_i^2 & \\ & & \ddots \end{bmatrix} \begin{bmatrix} H_{11}(\omega_1) & H_{12}(\omega_1) & \cdot & \cdot & H_{1n}(\omega_1) \\ H_{11}(\omega_2) & H_{12}(\omega_2) & \cdot & \cdot & H_{1n}(\omega_2) \\ \cdot & \cdot & \cdot & \cdot & \cdot \\ \cdot & \cdot & \cdot & \cdot & \cdot \\ H_{11}(\omega_n) & H_{12}(\omega_n) & \cdot & \cdot & H_{1n}(\omega_n) \end{bmatrix}_T \begin{bmatrix} M_{11} & M_{12} & \cdot & \cdot & M_{1n} \\ M_{21} & M_{22} & \cdot & \cdot & M_{2n} \\ \cdot & \cdot & \cdot & \cdot & \cdot \\ \cdot & \cdot & \cdot & \cdot & \cdot \\ M_{n1} & M_{n2} & \cdot & \cdot & M_{nn} \end{bmatrix}. \quad (11)$$

If the left-side term $[H]_T$ is $[A]$ and the right-side term is $[B]$

$$[A][K]_T = [B]. \quad (12)$$

The solution of Eq. (12), $[K]_T = ([A]^{\mathrm{T}}[A])^{-1}[A]^{\mathrm{T}}[B]$ using the least-squares method, will give the unknown value $[K]_T$. However, in our case, the determinant of $[A]^{\mathrm{T}}[A]$ is usually close to zero; thus, a different approach is required.

When we take the inverse matrix and consider the properties of the stiffness matrix elements that are distributed near the diagonal, we can reduce the unknown values and required FRFs for a general structure. For example, if we use only two elements that exist in the first column of the $[K]$ matrix, and make use of the fact that the mass $[M]$ is a diagonal matrix for static structures, from Eq. (11) we obtain

$$\begin{bmatrix} H_{11}(\omega_1) & H_{12}(\omega_1) \\ H_{11}(\omega_2) & H_{12}(\omega_2) \\ H_{11}(\omega_3) & H_{12}(\omega_3) \\ \vdots & \vdots \\ H_{11}(\omega_n) & H_{12}(\omega_n) \end{bmatrix} \begin{bmatrix} K_{11} \\ K_{21} \end{bmatrix} = \begin{Bmatrix} 1 + \omega_1^2 H_{11}(\omega_1) M_{11} \\ 1 + \omega_2^2 H_{11}(\omega_1) M_{11} \\ 1 + \omega_3^2 H_{11}(\omega_1) M_{11} \\ \vdots \\ 1 + \omega_n^2 H_{11}(\omega_1) M_{11} \end{Bmatrix}. \quad (13)$$

Thus, we can identify all the non-zero stiffness values using just a few FRFs in one row of the FRF matrix.

The discrete system model was used again to verify this method. The structure was assumed to be damaged at several locations. In the FRF matrix, the first row was used repeatedly for various frequency values. The largest error was determined by comparing the FRF before and after the damage. The least-squares method of Eq. (13) was used to calculate the reduction of the stiffness values. The identified stiffness reductions were the same as the assumed damage values in the discrete model.

Although this method gave accurate estimations of the damage for this case, it does not work well for some other cases. For example, when the columns in matrix $[A]$ have the same values, the damage estimations are incorrect. Although the orders of the elements in the $i$th and $j$th columns of the stiffness matrix are different from each other, they have a similar constitution that has same element

values such as $[0 \quad 0 \quad 0 \quad -10^6 \quad 2\times10^6 \quad -10^6]^{\mathrm{T}}$ and $[0 \quad 0 \quad 0 \quad -10^6 \quad -10^6 \quad 2\times10^6]^{\mathrm{T}}$ in the simple discrete model with six degrees of freedom. This gives the same FRF values using either Eq. (8) or Eq. (9).

The above method cannot be applied to general structures that have the same element material property, type, and size throughout, as is the case in some analysis models. For example, in a uniform beam model, the stiffness matrices of each element are equal. The same element matrices are superimposed to obtain the global stiffness matrix. Since we use only one specific row of FRFs, the values that are obtained from the matrix multiplication are equal even though the element values are different from each other. To overcome this problem, we concentrated on changes in the stiffness matrix caused by damage.

In Eqs. (8) and (9), if we assume that the mass of the structure remains constant before and after the damage, the change in the stiffness as a result of the damage is $[\Delta K] = [K]_A - [K]_T = [H]_A^{-1} - [H]_T^{-1}$. When multiplied by $[H]_T$, this yields

$$[H]_T[\Delta K] = [H]_T([K]_A - \omega^2[M]) - [I], \tag{14}$$

where $[H]_A$ can be calculated with using $[K]_A$ and $[M]$. If we assume that we can measure the first row of the FRF matrix to obtain the specific frequency, the above equation can be rearranged as follows:

$$\begin{aligned}
&[H_{T_{11}} \quad H_{T_{12}} \quad \cdots \quad H_{T_{1n}}]_T \begin{bmatrix} \Delta K_{11} & \Delta K_{12} & \cdots & \Delta K_{1n} \\ \Delta K_{21} & \Delta K_{22} & \cdots & \Delta K_{2n} \\ \vdots & \vdots & \ddots & \vdots \\ \Delta K_{n1} & \Delta K_{n2} & \cdots & \Delta K_{nn} \end{bmatrix} \\
&= [H_{T_{11}} \quad H_{T_{12}} \quad \cdots \quad H_{T_{1n}}]_T \begin{bmatrix} H_{A_{11}} & H_{A_{12}} & \cdots & H_{A_{1n}} \\ H_{A_{21}} & H_{A_{22}} & \cdots & H_{A_{2n}} \\ \vdots & \vdots & \ddots & \vdots \\ H_{A_{n1}} & H_{A_{n2}} & \cdots & H_{A_{nn}} \end{bmatrix}_A^{-1} - \begin{bmatrix} 1 & 0 & \cdots & 0 \end{bmatrix},
\end{aligned} \tag{15}$$

where $[\Delta K]$ is the change in the stiffness value of the damaged elements.

The previous methods detected damage in structures using modal test data and element-by-element adjustments to the FE model. In this method, the following element equations of the mass and stiffness matrices are used in a beam model to minimize the number of unknowns in the stiffness matrix and to preserve the intrinsic FEM connectivity properties of the model [13]

$$[K]_e = \frac{EI}{L^3}\begin{bmatrix} 12 & 6L & -12 & 6L \\ 6L & 4L^2 & -6L & 2L^2 \\ -12 & -6L & 12 & -6L \\ 6L & 2L^2 & -6L & 4L^2 \end{bmatrix},$$

$$[M]_e = \frac{\rho AL}{420}\begin{bmatrix} 156 & 22L & 54 & -13L \\ 22L & 4L^2 & 13L & -3L^2 \\ 54 & 13L & 156 & -22L \\ -13L & -3L^2 & -22L & 4L^2 \end{bmatrix}, \tag{16}$$

where $E$, $I$, $L$, $\rho$, and $A$ are Young's modulus, area moment of inertia, length of the beam element, density, and cross-sectional area, respectively. Separating the $EI$ values from Eq. (16) to reduce the number of variables and to maintain the physical meaning of the stiffness matrix yields

$$[K]_e = EI\left(\frac{1}{L^3}\begin{bmatrix} 12 & 6L & -12 & 6L \\ 6L & 4L^2 & -6L & 2L^2 \\ -12 & -6L & 12 & -6L \\ 6L & 2L^2 & -6L & 4L^2 \end{bmatrix}\right) = EI[K']_e, \tag{17}$$

where $[K']_e$ can be calculated using a finite element model. From the $1 \times n$ row on the right side of Eq. (15), if a value exists in the $i$th column then the stiffness value corresponding to the $i$th column element of $[\Delta K]$ will be changed. The $[K']_e$ value in Eq. (17) is known; only the $EI$ values are unknown. Thus, Eq. (15) becomes

$$([H]_T)_{xn} \times [K']_{(:,i)} \times \Delta(EI) = ([H]_T)_{xn} \times ([H]_A)^{-1}_{(:,i)} - [I]_{(x,i)}, \tag{18}$$

where $([H]_T)_{xn}$ is the $x$th row in the FRF matrix that was obtained from the test, $[K']_{(:,i)} \times \Delta(EI)$ is used to apply Eq. (17) to the $i$th column of $[\Delta K]$ in Eq. (15), and $([H]_A)^{-1}_{(:,i)} = ([K]_A - \omega^2[M])^{-1}_{(:,i)}$. If we let the known values of the left side of Eq. (18) be $\alpha(x,i)$ and the known values on the right side be $\beta(x,i)$, we have

$$\Delta(EI) = \beta(x,i)/\alpha(x,i). \tag{19}$$

Thus, we can calculate the change in stiffness due to structural damage by using calculated $\Delta(EI)$ values.

## 4. Numerical examples

### 4.1. Example 1: cantilever with and without cracks

In this section, the damage detection method was applied to a simple cantilever beam system. For the system model shown in Fig. 4, the FRFs can be obtained from an experiment with the physical model. However, representative FRFs were synthesized numerically using the continuous system model instead. It was assumed that the structure can be modelled using the finite element method with basic structural elements (i.e., bars, beams, plates, membranes, and shells). It was also assumed that the damage size is the same as the element size.

In the cantilever, $E = 3 \times 10^7$ psi, $L = 30$ in, $I = 0.0833\,\text{in}^4$, $A = 1\,\text{in}^2$, and $\rho = 0.00073\,\text{lb}\,\text{s}^2/\text{in}$. The model had 10 elements. The stiffness and mass matrices were obtained by superimposing Eq. (16). Since the cantilever had a fixed boundary condition at the left end, the first and the second rows and columns were eliminated from the $22 \times 22$ matrix, as we are concerned only with

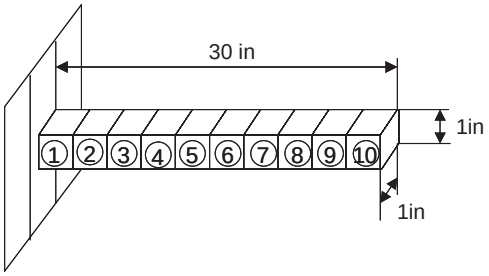


Fig. 4. Cantilever beam model.

transverse displacements and rotations. Hence, the following $20 \times 20$ stiffness matrix $[K]_A$ and mass matrix $[M]$ were created

$$[K]_A = 1 \times 10^6 \begin{bmatrix} 2.2213 & 0 & -1.1107 & 1.6660 & \cdots & 0 & 0 & 0 & 0 & 0 \\ 0 & 6.6640 & -1.6660 & 1.6660 & \cdots & 0 & 0 & 0 & 0 & 0 \\ -1.1107 & -1.6660 & 2.2213 & 0 & \cdots & 0 & 0 & 0 & 0 & 0 \\ 1.6660 & 1.6660 & 0 & 6.6640 & \cdots & 0 & 0 & 0 & 0 & 0 \\ 0 & 0 & -1.1107 & -1.6660 & \cdots & 0 & 0 & 0 & 0 & 0 \\ 0 & 0 & 1.6660 & 1.6660 & \cdots & 0 & 0 & 0 & 0 & 0 \\ \vdots & \vdots & \vdots & \vdots & \ddots & \vdots & \vdots & \vdots & \vdots & \vdots \\ 0 & 0 & 0 & 0 & \cdots & 1.6660 & 0 & 0 & 0 & 0 \\ 0 & 0 & 0 & 0 & \cdots & 1.6660 & 0 & 0 & 0 & 0 \\ 0 & 0 & 0 & 0 & \cdots & 0 & -1.1107 & 1.6660 & 0 & 0 \\ 0 & 0 & 0 & 0 & \cdots & 6.6640 & -1.6660 & 1.6660 & 0 & 0 \\ 0 & 0 & 0 & 0 & \cdots & -1.6660 & 2.2213 & 0 & -1.1107 & 1.6660 \\ 0 & 0 & 0 & 0 & \cdots & 1.6660 & 0 & 6.6640 & -1.6660 & 1.6660 \\ 0 & 0 & 0 & 0 & \cdots & 0 & -1.1107 & -1.6660 & 1.1107 & -1.6660 \\ 0 & 0 & 0 & 0 & \cdots & 0 & 1.6660 & 1.6660 & -1.6660 & 3.3320 \end{bmatrix}_{20\times20},$$

$$[M] = 1 \times 10^{-4} \begin{bmatrix} 16.269 & 0 & 2.8157 & -2.0336 & \cdots & 0 & 0 & 0 & 0 & 0 \\ 0 & 3.7543 & 2.0336 & -1.4079 & \cdots & 0 & 0 & 0 & 0 & 0 \\ 2.8157 & 2.0336 & 16.269 & 0 & \cdots & 0 & 0 & 0 & 0 & 0 \\ -2.0336 & -1.4079 & 0 & 3.7543 & \cdots & 0 & 0 & 0 & 0 & 0 \\ 0 & 0 & 2.8157 & 2.0336 & \cdots & 0 & 0 & 0 & 0 & 0 \\ 0 & 0 & -2.0336 & -1.4079 & \cdots & 0 & 0 & 0 & 0 & 0 \\ \vdots & \vdots & \vdots & \vdots & \ddots & \vdots & \vdots & \vdots & \vdots & \vdots \\ 0 & 0 & 0 & 0 & \cdots & -2.0336 & 0 & 0 & 0 & 0 \\ 0 & 0 & 0 & 0 & \cdots & -1.4079 & 0 & 0 & 0 & 0 \\ 0 & 0 & 0 & 0 & \cdots & 0 & 2.8157 & -2.0336 & 0 & 0 \\ 0 & 0 & 0 & 0 & \cdots & 3.7543 & 2.0336 & -1.4079 & 0 & 0 \\ 0 & 0 & 0 & 0 & \cdots & 2.0336 & 16.269 & 0 & 2.8157 & -2.0336 \\ 0 & 0 & 0 & 0 & \cdots & -1.4079 & 0 & 3.7543 & 2.0336 & -1.4079 \\ 0 & 0 & 0 & 0 & \cdots & 0 & 2.8157 & 2.0336 & 8.1343 & -3.4414 \\ 0 & 0 & 0 & 0 & \cdots & 0 & -2.0336 & -1.4079 & -3.4414 & 1.8771 \end{bmatrix}_{20\times20}.$$

We assumed that stiffness value was altered from $E = 3 \times 10^7$ to $2 \times 10^7$ psi due to damage at the 3rd, 4th, and 9th elements of the model. The stiffness matrix $[K]_T$ that was necessary to simulate the test FRF was obtained from Eq. (16). The mass matrix was assumed to be equal to the analytical values. Using these matrices, the FRFs were calculated from Eqs. (8) and (9). Note that the FRF in Eq. (9) should be obtained from an actual test rather than from the simulated values used in this example.

Two FRF values in one row of the global FRF matrix were used, corresponding to two elements with stiffness values. The FRF was assumed to have been measured at a test frequency of 3000 rad/s. Using the first row of the global matrix, the value $\beta(1, i)$ in Eq. (19) was

$$\begin{aligned}\beta(1,i) = [&0.0 \quad 0.0 \quad 0.0279 \quad 0.3813 \quad 0.0469 \quad -0.0044 \quad -0.0748\\ &-0.0687 \quad -0.0 \quad -0.0 \quad 0.0 \quad 0.0 \quad 0.0 \quad 0.0\\ &-0.0654 \quad -0.3018 \quad 0.0654 \quad 0.1056 \quad 0.0 \quad -0.0]_{1\times 20}.\end{aligned}$$

Here, the 3rd to the 8th and the 15th to the 18th elements had non-zero values. If the cantilever beam were undamaged, all values of $\beta(1, i)$ would be zero. If we consider the properties of Eq. (16), we can determine that the 3rd, 4th, and 9th components are damaged. Also, we can calculate the decrease in $EI$ values using Eqs. (18) and (19). By taking independent values that are not superimposed, we can obtain the reduction in the stiffness value of $EI = 8.33 \times 10^5\,\mathrm{lb\,m^2}$, which corresponds to $\beta(1, 3) = 0.0279$ in the 3rd element, $\beta(1, 8) = -0.0687$ in the 4th element, and $\beta(1, 15) = -0.0654$ in the 9th element. If we assume that only the $E$ values were affected by the damage (the $I$ values of each element remain unchanged), we obtain $\Delta E = 1 \times 10^7$ psi, which was assumed initially.

Next, suppose that each element has a different amount of damage, i.e., the 3rd and 9th element stiffness values were changed from $E = 3 \times 10^7$ to $2 \times 10^7$ psi, and the 4th element stiffness value was changed to $E = 2.5 \times 10^7$ psi. Using the same procedure, and assuming the same 3000-rad/s frequency, the calculated $\beta$ values using the first row of the global FRF matrix are

$$\begin{aligned}\beta(1,i) = [&0.0 \quad 0.0 \quad 0.0288 \quad 0.3815 \quad 0.0004 \quad -0.1788 \quad -0.0292\\ &-0.0286 \quad -0.0 \quad -0.0 \quad 0.0 \quad 0.0 \quad 0.0 \quad 0.0\\ &-0.0621 \quad -0.2867 \quad 0.0621 \quad 0.1003 \quad 0.0 \quad -0.0]_{1\times 20}.\end{aligned}$$

From this, $\beta(1, 3) = 0.0288$, and the reduced stiffness value of the 3rd element is $EI = 8.33 \times 10^5\,\mathrm{lb\,m^2}$. Also, from $\beta(1, 8) = -0.0286$ and $\beta(1, 15) = -0.0621$, the reduced stiffness values of the 4th and 9th elements are $EI = 4.165 \times 10^5$ and $8.33 \times 10^5\,\mathrm{lb\,m^2}$, respectively. For a fixed value of $I = 0.0833\,\mathrm{in^4}$, the change in Young's modulus is $\Delta E = 1 \times 10^7$ psi for the 3rd and 9th elements, and $\Delta E = 0.5 \times 10^7$ psi for the 4th element. Therefore, using this proposed method, we can accurately find the location and the amount of damage in a structure.

### 4.2. Example 2: the helicopter rotor blade

The proposed method was also applied to the helicopter rotor blade shown in Fig. 5. The rotor blade had a length of 1100 mm. A VR-12 airfoil was used between 220 and 880 mm, and a VR-15 airfoil between 1036 and 1100 mm. A linear airfoil shape transition was assumed between 880 and 1036 mm.

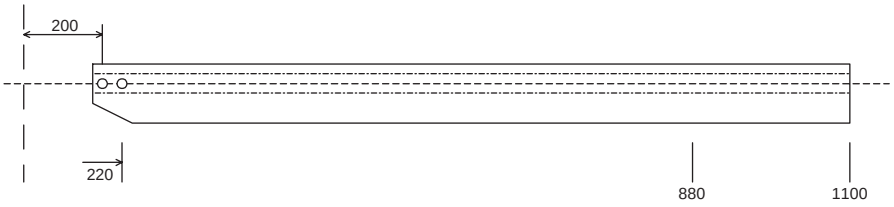


Fig. 5. Configuration of the rotor blade.

Table 1
Change in the natural frequency of the rotor blade due to damage (rad/s)

| Mode | Before damage | After damage |
|---|---|---|
| 1st | 2.7592e + 001 | 2.7012e + 001 |
| 2nd | 1.9023e + 002 | 1.8660e + 002 |
| 3rd | 5.3105e + 002 | 5.1870e + 002 |
| 4th | 1.0306e + 003 | 1.0164e + 003 |
| 5th | 1.7194e + 003 | 1.6850e + 003 |
| 6th | 2.5841e + 003 | 2.5052e + 003 |
| 7th | 3.5890e + 003 | 3.5424e + 003 |
| 8th | 4.7469e + 003 | 4.6331e + 003 |
| 9th | 6.0690e + 003 | 5.9033e + 003 |
| 10th | 7.5217e + 003 | 7.4423e + 003 |

The rotor blade was modelled as a cantilever beam since a simplified analysis is generally performed in the aircraft conceptual design phase. A total of 16 stiffness values were used, and the element masses were assumed to be concentrated at each node. A total of 42 beam elements were used so that $86 \times 86$ mass and stiffness matrices were constructed. Since fixed boundary conditions were applied at the root, the first and the second rows and columns were removed so that $84 \times 84$ mass and stiffness matrices remained.

The 3rd, 19th, and 24th elements were assumed to be damaged. The stiffness $EI$ of the 3rd element was reduced by 50% from 107.929 to 53.960 N m$^2$, the 9th element from 14.271 to 7.136 N m$^2$, and the 24th element from 14.271 to 10.000 N m$^2$. The changes in the natural frequencies are shown in Table 1. From the many FRFs, we chose to compare $H(1,4)$ of the damaged rotor blade to $H(1,4)$ of the undamaged rotor blade in Fig. 6.

Non-zero values of the $1 \times 84$ $\beta(1,i)$ vector obtained using this proposed method are listed in Table 2. These values indicate that the 3rd, 19th, and 24th elements are damaged. Using the same method as in the previous example, the identified change in stiffness of the 3rd, 19th, and 24th elements are $\Delta EI_3 = 53.9690$ N m$^2$, $\Delta EI_{19} = 7.1353$ N m$^2$, $\Delta EI_{24} = 4.2713$ N m$^2$. These values are exactly the same as the assumed values. Therefore, we conclude that this method of damage detection can be used for structures with damage at more than one location.

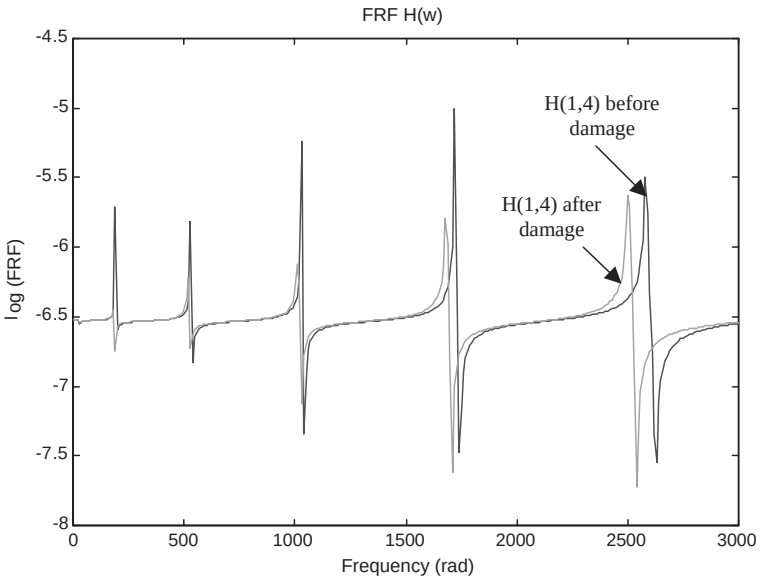


Fig. 6. Comparison of the H(1,4) FRF before and after damage.

Table 2
Non-zero $\beta(1,i)$ values of the $\beta(1,i)$ vector

| | | | | |
|---|---|---|---|---|
| Columns 3–6 | −0.0023 | 0.0001 | 0.0023 | −0.0001 |
| Columns 35–38 | −0.0015 | 0.0001 | 0.0015 | −0.0001 |
| Columns 45–48 | 0.0009 | 0.0000 | 0.0009 | 0.0000 |

## 5. Conclusions

In this paper, we developed damage detection methods that use FRFs to find the location and severity of damage in structures.

We started with a basic method that required a sharp increase in computational effort when the structure was damaged at more than one location. To overcome this problem, the least-squares method was used for different frequencies of a specific FRF; however, this was not satisfactory since the method encountered problems calculating the inverse of the matrices when the stiffness matrices had repeated elements. The best method identified structural damage using just a few FRFs. To minimize the number of unknowns, common stiffness variables were extracted from the finite elements. A few FRFs were sufficient to accurately identify the extent and location of the damage. The repeated use of a few FRFs for different frequency values, considering only a vector subset of the full set of FRFs, is the original work of this paper.

The required number of measured FRFs could be further reduced by using more constraint equations. Future research in this field should be focused on discovering the limitations of these methods using actual test data instead of simulated data. Also, geometric effects of damage directions must be investigated when modelling and testing for structural damage.

## Acknowledgements

This work was supported by a Korea Research Foundation Grant (KRF-99-003-E00104E1302).

## References

[1] M. Abdalla, K.M. Grigoriadis, D.C. Zimmerman, Enhanced damaged detection using linear matrix inequalities, Proceedings of the 16th International Modal Analysis Conference, Santa Barbara, CA, 1998, pp. 144–150.
[2] A.K. Pandey, M. Biswas, Damage detection in structures using changes in flexibility, Journal of Sound and Vibration 169 (1994) 3–17.
[3] C. Farhat, F.M. Hemez, Updating finite element dynamics models using an element-by-element sensitivity methodology, American Institute of Aeronautics and Astronautics Journal 31 (9) (1993) 1702–1711.
[4] P. Hajela, F.J. Soeiro, Structural damage detection based on static and modal analysis, American Institute of Aeronautics and Astronautics Journal 28 (6) (1990) 1110–1115.
[5] C. Li, S.W. Smith, Hybrid approach for damage detection in flexible structures, Journal of Guidance, Control, and Dynamics 18 (13) (1995) 419–425.
[6] H.T. Banks, D.J. Inman, D.J. Leo, Y. Wang, An experimentally validated damage detection theory in smart structures, Journal of Sound and Vibration 191 (1996) 859–880.
[7] S.W. Smith, Iterative matrix approximation for model updating, Mechanical Systems and Signal Processing 12 (1) (1998) 187–201.
[8] H. Ahmadian, J.E. Mottershead, M.I. Friswell, Regularisation methods for finite element model updating, Mechanical Systems and Signal Processing 12 (1) (1998) 47–64.
[9] S.W. Doebling, Rank optimal update of elemental stiffness parameters for structural damage identification, American Institute of Aeronautics and Astronautics Journal 34 (12) (1996) 2615–2621.
[10] J.S. Lew, Using transfer function parameter changes for damage detection of structures, American Institute of Aeronautics and Astronautics Journal 33 (11) (1995) 2189–2193.
[11] I. Sheinman, Damage detection and updating of stiffness and mass matrices using mode data, Computers and Structures 59 (1) (1996) 149–156.
[12] D. Li, Z. Zheng, K. He, B. Wang, Damage detection in offshore structures by the FRF method, Proceedings of the International Offshore Mechanics and Arctic Engineering, Calgary, Vol. 1, Part B, 1992, pp. 601–604.
[13] D.L. Logan, A First Course in the Finite Element Method, 2nd Edition, PWS, Boston, 1992.
[14] H.Y. Hwang, Identification techniques of structure connection parameters using frequency response functions, Journal of Sound and Vibration 212 (1998) 469–769.
[15] H.Y. Hwang, Identification Methods for Physical Parameters in Structure, Doctoral Thesis, Georgia Institute of Technology, Atlanta, GA, 1993.
[16] D.J. Ewins, Modal Testing: Theory and Practice, Research Studies Press, Letchworth, Hertfordshire, England, 1984.